Papers submitted to the Conference "Applications of Physics in Mechanical and Material Engineering"

Magnetic State of Martensite in $Ni_{48}Mn_{39.5}Sn_{12.5-x}Al_x$ $(x = 0, 1, 2, 3)$ Metamagnetic Shape Memory Alloy Ribbons

P. Czaja*

The Aleksander Krupkowski Institute of Metallurgy and Materials Science of the Polish Academy of Sciences, 25 Reymonta, 30-059 Kraków, Poland

Doi: 10.12693/APhysPolA.142.180 *e-mail: p.czaja@imim.pl

Melt spun $Ni_{48}Mn_{39.5}Sn_{12.5-x}Al_x$ $(x = 0, 1, 2, 3)$ ribbons undergoing a thermoelastic martensitic phase transition concomitant with an abrupt magnetization change were examined with respect to the magnetic response of the low-temperature martensite phase, which shows complex magnetism. It has been shown that in the intermediate temperature range between the martensite finish temperature and the Curie temperature of martensite, the intermediate state is weakly magnetic and is in part composed of a superparamagnetic phase. The average magnetic moment, probed by the modified Langevin model, weakens as the amount of Al increases in the alloys. This might be related to changes in the magnetic response of the parent austenite phase switching from ferromagnetic into paramagnetic, atomic order of which is inherited by the martensite phase. A quasi-magnetic phase diagram was established to trace the evolution of the magnetic response of the ribbons as a function of Al concentration and to aid composition optimisation for engineering applications.

topics: shape memory alloy, melt spun, magnetization

1. Introduction

The Ni–Mn–X (X = Ga, In, Sn) intermetallic alloys represent a unique class of external stimuli-responsive smart systems with an intrinsically complex and interrelated microstructure and magnetism [1]. For the past two decades, these systems have been widely researched for magnetic shape memory and multicaloric response, which both are afforded by a thermoelastic, reversible martensitic phase transformation [2]. This fist-order solid to solid phase transition proceeds from the cubic $L2_1$ ordered parent phase into a low temperature, lower symmetry than the parent, martensite state with a variety of modulated, i.e., 4O-, 10M-, 14M-, or non-modulated (NM) structures [3]. The magnetic moment in these systems is chiefly attributed to the Mn atoms, and their coupling takes place via the oscillatory Ruderman–Kittel–Kausya–Yosida interaction, mitigated through the polarization of the valence electrons, and is sensitive to an average atomic distance between the Mn atoms. Since the structural symmetry of the ferromagnetic $L2_1$ ordered parent phase collapses upon the transformation, its magnetism simultaneously undergoes profound alteration leading to the weakly magnetic or paramagnetic martensite phase. Upon continued cooling, below the martensite finish temperature, the low symmetry phase undergoes ferromagnetic ordering and, frequently at low temperatures, it can coexist with antiferromagnetic and/or superparamagnetic type phases [4]. Such coexistence of various magnetic phases may lead to magnetically inhomogeneous and frustrated states, giving rise to e.g. the spin glass type behaviour [5]. Aside from the fundamental interest in the physical intricacies of mixed magnetic states, magnetic inhomogeneity can also account for additional, functional phenomena like the exchange bias effect (EB) with potential for spin electronics and digital memory applications [6, 7]. It is hence worthwhile to examine the exact nature of the magnetic state at low temperatures in Ni–Mn-based magnetic shape memory alloys, which is not too often disseminated in the literature. In this contribution, the magnetic state of martensite at temperatures below the martensite finish temperatures is evaluated on the example of $Ni_{48}Mn_{39.5}Sn_{12.5-x}Al_x$ $(x = 0, 1, 2, 3)$ melt spun alloy system.

2. Materials and methods

Melt spun ribbons with the nominal composition of $Ni_{48}Mn_{39.5}Sn_{12.5-x}Al_x$ $(x = 0, 1, 2, 3)$ were produced by melt-spinning technique from induction cast master ingots. More details can be found elsewhere [8]. The structure, microstructure of the ribbons as well as their magnetocaloric behaviour have been examined before, see [9–12]. The DC mass susceptibility and magnetization were measured

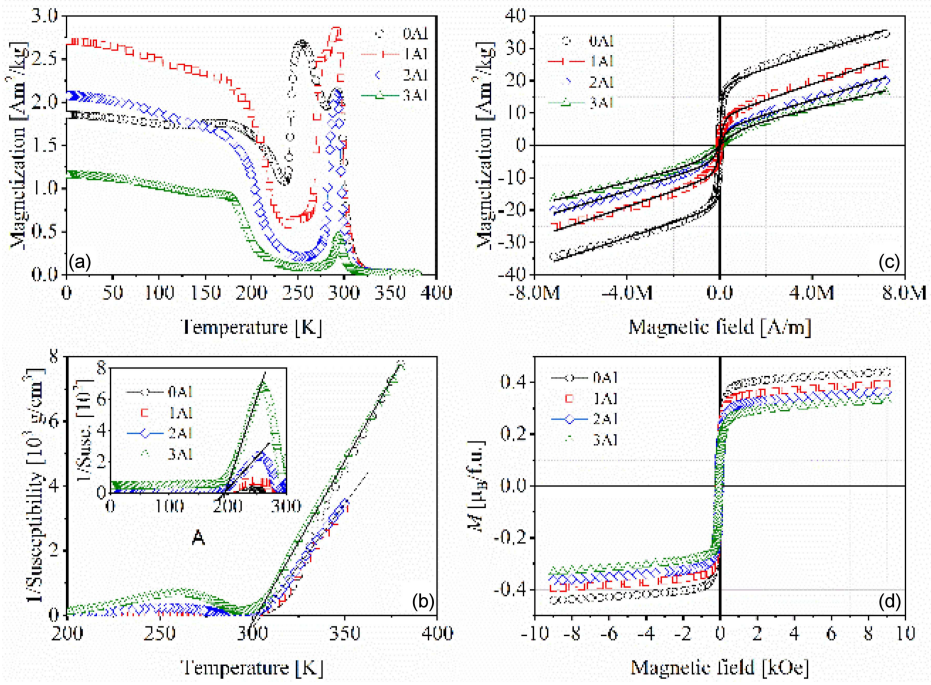

Fig. 1. Magnetization vs temperature (a), inverse susceptibility as a function of temperature (b), isothermal magnetization as a function of the applied magnetic field and measured at (c) 230, 255, 270 K and (d) 3 K for all the $Ni_{48}Mn_{39.5}Sn_{12.5-x}Al_x$ $(x = 0, 1, 2, 3)$ ribbons.

in the temperature range from 2 up to 380 K and in the magnetic fields up to 90 kOe using the vibrating sample magnetometer (VSM) option of the Quantum Design Physical Property Measurement System (PPMS-9). For measurements, the ribbons were crushed and pressed in cylindrical polypropylene sample holders.

3. Results

Figure 1a shows magnetization M versus temperature T recorded at 5 mT for all the $Ni_{48}Mn_{39.5}Sn_{12.5-x}Al_x$ $(x = 0, 1, 2, 3)$ ribbons. Regardless of the Al content, all four ribbons are paramagnetic above 300 K, and as the temperature decreases, they all undergo a martensitic transformation, evident from an abrupt magnetization change following the first Curie upturn. Seemingly at the intermediate stage between 200 and 300 K, the martensite phase is weakly magnetic. It shows nonzero magnetization, and eventually orders ferromagnetically at temperature below 200 K, i.e., well below the martensite finish temperatures. In order to probe whether both austenite and martensite are purely paramagnetic above their respective Curie temperatures, the Curie-Weiss (C-W) law

$$\chi = \frac{C}{T - T_{\mathrm{C}}} \quad \rightarrow \quad \frac{1}{\chi} = \frac{T}{C} - \frac{T_{\mathrm{C}}}{C} \tag{1}$$

was applied to the reciprocal of magnetic susceptibility (see Fig. 1b). In (1), χ, T_{C}, and C are the magnetic susceptibility, Curie temperature, and Curie constant, respectively. It was found that the inverse of the magnetic susceptibility vs temperature (Fig. 1b) shows linear behaviour, and the effective moments were determined according to following formula

$$C = \frac{N_{\mathrm{A}}}{3k_{\mathrm{B}}}\,\mu_0\mu_{eff}^2, \tag{2}$$

where N_{A} is the Avogadro's number, k_{B} is the Boltzmann constant and μ_0 is the vacuum permeability. The Curie temperatures determined from the fitting are given in Table I along with the established magnitudes of calculated μ_{eff}. The Curie temperatures are consistent with those obtained from the $M(T)$ dependence [8]. While the established μ_{eff} in austenite is largely in good agreement with literature in the case martensite, it shows somewhat excessive values indicating more complex magnetic exchange.

TABLE I

Effective magnetic moments (in $[\mu_{\mathrm{B}}/\mathrm{f.u.}]$) and Curie temperatures [K] obtained from the linear fit to the inverse susceptibility vs temperature curves for austenite and martensite in the $Ni_{48}Mn_{39.5}Sn_{12.5-x}Al_x$ $(x = 0, 1, 2, 3)$ melt spun alloys.

Alloy	$\mu_{eff}^{\mathrm{aust.}}$	$\mu_{eff}^{\mathrm{mart.}}$	$T_{\mathrm{C-W}}^{\mathrm{aust.}}$ [K]	$T_{\mathrm{C-W}}^{\mathrm{mart.}}$ [K]
0Al	2.6	–	305	193
1Al	3.3	15.9	302	194
2Al	3.1	11.0	300	193
3Al	2.3	7.8	300	187

TABLE II

Alloy composition, isothermal measurement temperature and the fitted parameters μ, N and χ determined from the Langevin fit of the isothermal $M(H)$ curves for martensite in the $Ni_{48}Mn_{39.5}Sn_{12.5-x}Al_x$ ($x = 0, 1, 2, 3$).

Alloy	T [K]	μ [μ_B/f.u.]	N [m^{-3}]	χ
0Al	230	8.3×10^3	2.5×10^{20}	2.3×10^{-6}
1Al	255	4.4×10^3	2.3×10^{20}	2.4×10^{-6}
2Al	270	2.4×10^3	2.5×10^{20}	2.1×10^{-6}
3Al	270	0.8×10^3	6.6×10^{20}	1.7×10^{-6}

Thus, the modified Langevin model was used to test the martensite phase within the intermediate temperature range for superparamagnetism. In line with the model, the macroscopic magnetization of a system composed of a number of particles with density N and the average magnetic moment μ can be described as follows

$$M(H) = N\mu L(\xi) + \chi H, \tag{3}$$

where $L(\xi) = \mathrm{cotanh}(\xi) - 1/\xi$ is the Langevin function of $\xi = \mu_0 \mu H/(k_B T)$ and χ is the magnetic susceptibility of the matrix. The fitting for each individual composition was performed at temperatures below the martensite finish temperature and above its respective martensite Curie temperature (Fig. 1c). On the whole, the curves conform to the Langevin law and show a reasonable fit as indicated in Fig. 1c by a solid, black line. On the whole, as evident in Table II, the average particle density N is comparable for all ribbons, while the average magnetic moment decreases with increasing Al content. The values are largely in agreement with the literature on similar systems [13] and suggest a superparamagnetic type behaviour. Accordingly, the shape of the curves is sigmoidal, and the state of saturation is not attained even despite an extensive magnetic field applied. These obtained results indicate a weakening ferromagnetic contribution in martensite at the intermediate temperature range when the content of Al increases.

The effect of decreasing magnetization following the addition of Al into the system can also be well traced from isothermal magnetization measurements performed at 3 K and shown in Fig. 1d. This is most likely due to the shrinkage of the unit cell volume discussed elsewhere [8].

In general, it appears that the martensite state in the intermediate temperature range above the Curie temperature of martensite and below the martensite finish temperature shows complex magnetism, in part attributable to the superparamagnetic exchange. The likely source of superparamagnetic contribution may be associated with the intrinsic properties of the martensite phase [14] or it may stem form the retained austenite fraction, which undergoes and preserves its own ferromagnetic ordering during cooling. The latter would justify the observed decrease in the average magnetic moment values more noticeable at a higher concentration of Al. As it is clear from previous studies [8], the introduction of Al results in an increase of the martensite start temperature while it has a limited effect on the Curie temperature of austenite, thus the magnetic nature of the transforming phases switches from ferro austenite → weak magnetic martensite into para austenite → weak magnetic martensite. Since the atomic ordering is inherited from the parent phase by martensite, so is its magnetic make up. Based on these results and previous analysis [8], a quasi-magnetic phase diagram can be constructed explaining the observed magnetization changes (see Fig. 2).

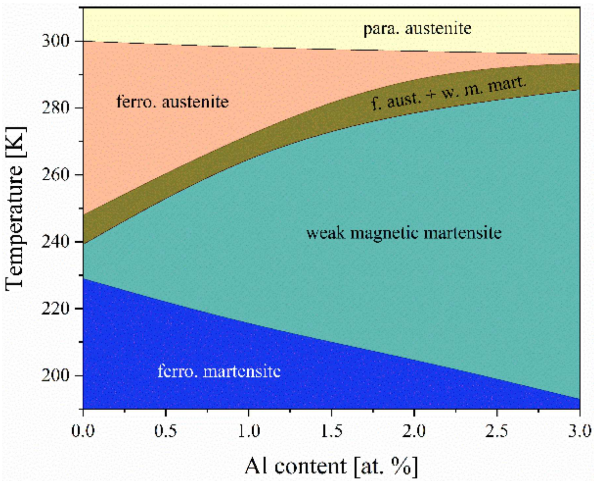

Fig. 2. Quasi magnetic phase diagram for the $Ni_{48}Mn_{39.5}Sn_{12.5-x}Al_x$ ($x = 0, 1, 2, 3$) system as a function of Al concentration.

4. Conclusions

The $Ni_{48}Mn_{39.5}Sn_{12.5-x}Al_x$ ($x = 0, 1, 2, 3$) melt spun ribbons capable of a reversible martensitic phase transformation were evaluated in terms of the magnetic behaviour of martensite in the intermediate temperature range below the martensite finish temperature and above the Curie temperature of martensite. It appears that the weak magnetic martensite is in part composed of the superparamagnetic phase and, interestingly, the average magnetic moment decreases with increasing Al concentration. The coincides with the change in the nature of the parent phase, which switches from ferromagnetic austenite to paramagnetic austenite as the level of Al increases.

Acknowledgments

The Aleksander Krupkowski Institute of Metallurgy and Materials Science of the Polish Academy of Sciences is gratefully acknowledged for support.

References

[1] A. Planes, Ll. Manosa, M. Acet, *J. Phys.: Condens. Matter* **21**, 233201 (2009).

[2] X. Moya, Ll. Manosa, A. Planes, T. Krenke, M. Acet, E.F. Wassermann, *Mat. Sci. Eng. A* **438-440**, 911 (2006).

[3] Y. Sutou, Y. Imano, N. Koeda, T. Omori, R. Kainuma, K. Ishida, K. Oikawa, *Appl. Phys. Lett.* **85**, 4358 (2004).

[4] D.Y. Cong, S. Roth, Y.D. Wang, *Phys. Status Solidi B* **251**, 2126 (2014).

[5] S. Chatterjee, S. Giri, S.K. De, S. Majumdar, *Phys. Rev. B* **79**, 092410 (2009).

[6] Y.B. Yanq, X.B. Ma, X.G. Chen, J.Z. Wei, R. Wu, J.Z. Han, H.L. Du, C.S. Wang, S.Q. Liu, Y.C. Yang, Y. Zhang, J.B. Yang, *J. Appl. Phys.* **111**, 07A916 (2012).

[7] M. Khan, I. Dubenko, S. Stadler, N. Ali, *J. Appl. Phys.* **102**, 113914 (2007).

[8] W. Maziarz, P. Czaja, M.J. Szczerba, J. Przewoźnik, C. Kapusta, A. Żywczak, T. Stobiecki, E. Cesari, J. Dutkiewicz, *J. Magn. Magn. Mater.* **348**, 8 (2013).

[9] P. Czaja, W. Maziarz, J. Przewoźnik, C. Kapusta, L. Hawelek, A. Chrobak, P. Drzymała, M. Fitta, A. Kolano-Burian, *J. Magn. Magn. Mater.* **358-359**, 142 (2014).

[10] P. Czaja, W. Maziarz, J. Przewoźnik, A. Żywczak, P. Ozga, M. Bramowicz, S. Kulesza, J. Dutkiewicz, *Intermetallics***55**, 1 (2014).

[11] P. Czaja, M. Fitta, J. Przewoźnik, W. Maziarz, J. Morgiel, T. Czeppe, E. Cesari, *Acta Mater.* **103**, 30 (2016).

[12] P. Czaja, J. Przewoźnik, M. Fitta, *Mater. Res. Bull.* **135**, 111120 (2020).

[13] C. Segui, E. Cesari, P. Lazpita, *J. Phys. D: Appl. Phys.* **49**, 165007 (2016).

[14] P. Czaja, J. Przewoźnik, R. Chulist, *J. Magn. Magn. Mater.* **514**, 167190 (2020).